Int J Clin Exp Med 2018;11(11):11743-11752
www.ijcem.com /ISSN:1940-5901/IJCEM0078462

Original Article

Regulatory mechanisms of miR-96-mediated AKT/mTOR signaling pathways for non-alcoholic steatohepatitis

Ping Tian[1*], Bei Sun[1*], Xiancheng Ma[1], Xidong Li[2], Enqin Liu[2], Likun Wang[2]

[1]The Eleventh Clinical Medical College of Qingdao University (Linyi People's Hospital), Linyi, Shandong Province, China; [2]Department of Infectious Diseases, Linyi People's Hospital, Linyi, Shandong Province, China. [*]Equal contributors and co-first authors.

Received April 24, 2018; Accepted July 14, 2018; Epub November 15, 2018; Published November 30, 2018

Abstract: Objective: The aim of this study was to discuss regulatory mechanisms of microRNA-96 (miR-96)-mediated AKT/mTOR signaling pathways for non-alcoholic steatohepatitis (NASH). Methods: Twenty-four male specific pathogen-free C57BL/6J mice were randomly divided into a control group (n=12, normal diet) and NASH model group (n=12, high-fat diet). Liver tissue samples of the two groups were collected and immunohistochemistry was used to detect expression of mTOR. A NASH cell model was established. Mice were divided into 4 groups, including the blank group, negative control (NC) group, miR-96 mimic group, and miR-96 inhibitor group. Dual-luciferase reporter assays were used to verify the targeting relationship between miR-96 and mTOR. qRT-PCR was used to detect expression of miR-96 in liver tissues of each group and expression of mRNA in the cells of each group. Western blot, MTT, and Hoechst staining were used to detect protein expression, cell proliferation, and apoptosis of each group. Results: Compared to the control group, miR-96 expression was increased in the NASH model group, while mTOR expression significantly decreased (both $P<0.05$). Compared to the blank group and NC group, expression of miR-96 mRNA was significantly increased in the miR-96 mimic group, mTOR, AKT, and S6K1 mRNA and protein levels and their phosphoprotein levels were significantly decreased, cell proliferation rate was significantly increased, and apoptosis rate was lower (all $P<0.05$). In the miR-96 inhibitor group, expression of miR-96 mRNA was significantly decreased, mTOR, AKT, and S6K1 mRNA and protein levels and their phosphoprotein levels were significantly increased, cell proliferation rate was significantly decreased, and apoptosis rate was higher (all $P<0.05$). Conclusion: High expression of miR-96 can inhibit AKT/mTOR signaling pathways, promote proliferation of non-alcoholic hepatitis cells, and reduce apoptosis.

Keywords: microRNA-96, AKT/mTOR, signaling pathways, non-alcoholic steatohepatitis, HL-7702 cells

Introduction

Non-alcoholic steatohepatitis (NASH) is a clinical commonly acquired metabolic stress-induced liver injury disease [1]. NASH occurrence has been associated with hepatic lipodystrophy, oxidative stress, lipid peroxidation injury, accumulation of free fatty acids (FFA), and heredity. NASH may further develop into liver fibrosis, liver cirrhosis, or liver cancer [2, 3]. Hepatocellular necrosis, with or without liver fibrosis, and inflammatory cell infiltration are pathological features of NASH [4].

MicroRNA (miRNA) molecules play an important role in regulating biological activities of cells. Most miRNAs are characterized by tissue-specificity and high temporality. They also participate in proliferation and differentiation of cells in the human body [5, 6]. In recent years, several studies on microRNA-96 (miR-96) found that miR-96 has abnormal expression in many malignant tumors, suggesting that miR-96 plays a key role in the development of malignant tumors [7-9]. miR-96 is expressed in a variety of human cells, including osteoblasts and adipose tissue. It plays a conspicuous role in the differentiation and development of tissues and organs and the maintenance of normal functions [10]. Other studies have found that miR-96 function inhibitors play an important role in the prevention and treatment of dis-

eases, including hyperlipidemia and fatty liver [11].

This present study proved that Akt/mTOR signaling pathways play important roles in a variety of malignant tumors. They can regulate growth, transcription, apoptosis, metabolism, and other biological processes of cells. They are a controller of cell growth, proliferation, survival, and differentiation. They play an important role in physiological and pathological processes [12]. In recent years, one study also found that Akt/mTOR signaling pathways may be associated with onset of NASH. An animal study showed that, after inhibition of Akt/mTOR signaling pathways, the effects of treating rats with liver fat-regulating agents was poor and proliferation of non-alcoholic hepatitis cells was further enhanced [13]. This suggests that Akt/mTOR signaling pathways are correlated with onset of NASH. However, there are few studies at present. It is impossible to elucidate the specific correlation.

This present study aimed to discuss regulatory mechanisms of miR-96-mediated AKT/mTOR signaling pathways for NASH.

Methods

Experimental animals

Twenty-four male specific pathogen-free C57BL/6J mice (age: 4 weeks, weight: 18-20 g) were purchased from Experimental Animal Center of Zhejiang Academy of Medical Sciences. They were habituated to their new environment for one week before the experiment. This experimental procedure and animal use plan was approved by the Animal Ethics Committee of The First Affiliated Hospital of Zhejiang University School of Medicine. All animal experiments followed the Declaration of Helsinki.

Construction of mice model of NASH

Twenty-four mice were randomly divided into two groups, the control group (n=12) and NASH model group (n=12). All mice were all raised at the Experimental Animal Center of The First Affiliated Hospital of Zhejiang University School of Medicine (experimental animal use license number: SYXK(Z)2013-0180). Mice in the control group were fed a normal diet. Mice in the NASH model group were fed a high-fat diet (purchased from Johnson & Johnson) [14].

Sample collection

Before the mice were sacrificed, they were fasted overnight. After weighing the next day, they were sacrificed by collecting arterial blood from the eyeballs. The wet weight of the liver was measured and one liver tissue was cut from the left middle lobe of the liver. Tissues were fixed with formalin (10%), conventionally dehydrated, embedded in paraffin, and sliced. After rinsing with 4°C PBS solution, they were stored in liquid nitrogen for future use [15].

Dual-luciferase reporter assay

Complete sequences of miR-96 and mTOR were obtained from the gene database (http://www.ncbi.nlm.nih.gov/gene). The full length and 3'UTR region of mTOR were cloned and amplified into pmirGLO Luciferase vector (E1330, Promega, USA), which was named pmTOR-Wt. Biological information software was used to predict the site-directed mutation at the binding site of miR-96 and mTOR. pmTOR-Mut vector was constructed. Internal control was the pRL-TK vector expressing Renilla luciferase (E2241, Promega, USA). miR-96 mimics and miR-96 negative control (NC) were separately co-transfected into HL-7702 cells (Shanghai Institute of Cell Biology, Chinese Academy of Sciences) together with luciferase reporter vector by Lipofectamine 2000 transfection reagent. Fluorescence intensity was detected by a fluorescence detector (Glomax 20/20, Promega, USA). All of the above plasmids were purchased from Addgene, USA. This experiment was repeated three times.

Establishment of cell model of NASH

Human normal hepatocyte cell line HL-7702 was provided by Shanghai Institute of Cell Biology, Chinese Academy of Sciences. Cells were incubated at 37°C in a 5% CO_2 incubator. When the cells became adherent, they were placed in 1 mM FFA high-fat medium and incubated at 37°C in a 5% CO_2 incubator for 24 hours [14].

Cell transfection and grouping

Cells were divided into 4 groups: blank group (modeled cells), NC group (modeled cells transfected with empty vector plasmids), miR-96 mimic group (transfected with miR-96 mimic plasmids), and miR-96 inhibitor group (transfected with miR-96 inhibitor plasmids). The

Table 1. qRT-PCR primer sequences

Gene	Sequence
miR-96	Upstream: 5'-CGGCGGTTTGGCACTAGCACATT-3'
	Downstream: 5'-CAGTGCGTGTCGTGGAGT-3'
AKT	Upstream: 5'-TTTATTGGCTACAAGGAACG-3'
	Downstream: 5'-AGTCTGAATGGCGGTGGT -3'
mTOR	Upstream: 5'-ATGCTTGGAACCGGACCTG-3'
	Downstream: 5'-TCTTGACTCATCTCTCGGAGTT-3'
S6K1	Upstream: CGTGGAGTCTGCGGCGGGTC
	Downstream: CGCTCTGCTTTCGTGTGGGC
GAPDH	Upstream: 5'-CACGGCAAGTTCAACGGCACAGTCA-3'
	Downstream: 5'-GTGAAGACGCCAGTAGACTCCACGAC-3'
U6	Upstream: 5'-GCTTCGGCAGCACATATACTAAAAT-3'
	Downstream: 5'-CGCTTCACGAATTTGCGTGTCAT-3'

Note: miR-96, microRNA-96.

above plasmids were purchased from Shanghai GenePharma Co., Ltd. Logarithmic-phase cells were digested, centrifuged, and counted. They were seeded at $2*10^3$ cells/well in a 96-well plate. After adjusting the cell concentration to $3*10^5$ cells/mL, the cells were further incubated for 24 hours at 37°C in a 5% CO_2 incubator. When cell density reached about 70%, the empty vector plasmids, miR-96 mimic plasmids, and miR-96 inhibitor plasmids were transfected into the cells with Lipofectamine™ 2000 and incubated for another 48 hours in l mM FFA high-fat medium. Cells were then collected for follow up experiments.

qRT-PCR testing

According to TRIzol instructions (Thermo Fisher Scientific, USA), total RNA was extracted from the cells and tissues. Concentration and purity of RNA were tested by UV spectrophotometry (UV1901, Beijing Mairuibo Biotechnology Co., Ltd.). The concentration of the sample with the purity of 1.8-2.0 (=A260/A280) was adjusted to 50 ng/μL. RNA was reverse-transcribed into cDNA (50 ng/μL) with the PrimeScriptTM RT reagent kit (Takara, RR047A, Beijing Think-Far Technology Co., Ltd.) and stored at -80°C for future use. Primers were designed using gene tool software and primer synthesis was completed by Annoron (Beijing) Biotechnology Co., Ltd. (**Table 1**).

According to ABI 7900HT real-time quantitative PCR two-step methods, GAPDH and U6 were set as internal controls. Reaction conditions were: pre-denaturation at 95°C for 30 seconds, denaturation at 95°C for 5 seconds, annealing at 58°C for 30 seconds, and extension at 72°C for 15 seconds, for a total of 40 cycles. Relative expression levels of miR-96, AKT, mTOR, and S6K1 mRNAs were calculated by the $2^{-\Delta\Delta Ct}$ method and each sample had 3 parallel holes for each gene. The experiment was repeated three times.

Western blotting

Total protein was extracted using a protein extraction kit (Bestbio, Shanghai). Protein concentrations of each sample were determined using a BCA kit (23225, Pierce, USA). A total of 10% SDS-PAGE gel (P0012A, Beyotime Institute of Biotechnology) was prepared. Protein samples (50 μg) were added to each well and electrophoresed at constant voltage of 80 V and 120 V, separately. After 2 hours of agarose gel electrophoresis, the protein was transferred to PVDF membranes (ISEQ00010, Millipore, Billerica, MA, USA) by the wet transfer method. The gel was electrophoretically transferred to a membrane at 250 mA for 90 minutes. PVDF membrane was blocked in TBST (containing 5% skim milk powder) for 2 hours and then washed with TBST. Mouse anti-human primary antibodies (mTOR (ab2732), p-mTOR (ab109268), AKT (ab8805), p-AKT (ab38449), S6K1 (ab32529), p70S6K1 (ab2571), GAPDH (ab181602), all purchased from Abcam, Cambridge, UK) were added dropwise and incubated at 4°C overnight. Next, the membrane was washed 10 minutes each time with TBST for a total of three times. It was incubated for 1 hour with peroxidase-conjugated Goat anti-Mouse IgG (HA1003, Yanhui Biotechnology Co., Ltd.) secondary antibody at room temperature. After washing with TBST for 10 minutes, three times, the PVDF membrane was visualized in the ECL reaction solution (WBKLS0100, Millipore). It was developed after exposure in a cassette. Using GAPDH as an internal control, relative expression of protein = gray value of target band/gray value of internal control band. The experiment was repeated three times.

Immunohistochemistry

Five paraffin sections from each group were deparaffinized twice with xylene for 3 minutes

each time. They were then dehydrated with graded ethanol. Sections were soaked in 3% H_2O_2 for 10 minutes and washed in distilled water. After 3 minutes of antigen retrieval under high pressure, sections were cooled to room temperature and washed with PBS three times for 3 minutes each. After adding 100 μL of 5% BSA blocking buffer, sections were incubated at 37°C for 30 minutes. After adding 100 μL of mTOR antibody (Abcam, ab32572, 1:1000), sections were incubated at 4°C overnight. Sections were washed with PBS three times for 3 minutes each. After adding 1:100 Biotin-conjugated Goat Anti-Rabbit IgG (HY90046, Shanghai Hengyuan Biological Technology Co., Ltd., Shanghai, China) secondary antibody, sections were incubated for 30 minutes at 37°C. After washing with PBS, sections were transferred to a streptomycin anti-biotin-peroxidase solution and incubated at 37°C for 30 minutes. Sections were washed with PBS three times for 3 minutes each. Sections were visualized in DAB at room temperature, soaked in hematoxylin for 5 minutes, and washed with running tap water. Sections were dipped in 1% hydrochloric acid-alcohol solution for 5 seconds and blued in running tap water for 20 minutes. Immunohistochemical results were analyzed under a high-powered lens by Image-Proplus software (Media Cybernetics, USA). Brown-yellow granules in the cytoplasm represented positive expression of mTOR protein. Five high-power fields were selected randomly from each section. Additionally, 100 cells were selected from each field and the positive expression of protein was judged from the percentage of positive cells. Results were negative if expression of positive cells was lower than 10%. Results were positive if expression of positive cells was higher than 10% and lower than 50%. Results were strong positive if expression of positive cells was higher than 50%. The experiment was repeated three times.

Proliferation of MTT test cells

HL-7702 cells in the logarithmic phase after transfection were taken from each group. The cells were suspended in a centrifuge tube and evenly blown using a sterile pipette. Viable cell count was calculated after trypan blue staining. Viable cells were seeded at $1*10^4$ cell/well in a 96-well plate, 0.2 mL per well. Next, the plate was incubated at 37°C in a 5% CO_2 incubator for 48 hours. After the plate was taken out, 20 μL of solution containing 5% MTT was added to each well. After mixing, the plate was incubated at 37°C in a 5% CO_2 incubator for 4 hours. The plate was taken out and centrifuged at 1,000 rpm for 10 minutes. After removal of the supernatant, 100 μL of DMSO was added to each well in the dark. The crystals were fully dissolved by slow-speed oscillation for 10 minutes. After removing the plate, optical density (OD) was measured at a wavelength of 570 nm by ELISA reader (SAF-680T, Multiskan GO, Thermo, USA) (ranging from 0.75 to 1.25). A cell growth curve was plotted with MTT treatment time as the horizontal axis and OD value as the vertical axis. The experiment was repeated three times.

Hoechst staining

Logarithmic-phase cells were digested with 0.25% trypsin-0.02% EDTA solution. Cells were centrifuged, resuspended, and seeded at $6*10^5$ cells/mL in a 24-well plate, 500 μL per well. Next, the plate was incubated at 37°C in a 5% CO_2 incubator for 24 hours. Each group had 4 parallel holes. When the cells became adherent, the coverslip was removed. They were washed with PBS three times for 3 minutes each. Cells were stained with Hoechst 33258 solution (C1011, Beyotime) for 10 minutes. After staining, five high-power fields were selected. Brightening, pyknosis, and concentration of apoptotic nuclei were found under a high-powered lens. Apoptosis rate was calculated as follows: apoptosis rate = number of positive cells/total number of cells * 100%. The experiment was repeated three times.

Statistical analysis

Statistical analysis was performed using SPSS19.0 statistical software and all experiments were repeated three times. Measurement data are presented as mean ± standard deviation. t-test was used to compare normally-distributed measurement data of two groups and one-way ANOVA was used to compare among multiple groups, expressed by F. Statistical significance is set at $p<0.05$.

Results

Verification results of targeting relationship between miR-96 and mTOR

Analysis by on-line analysis software revealed the existence of binding sites between miR-96

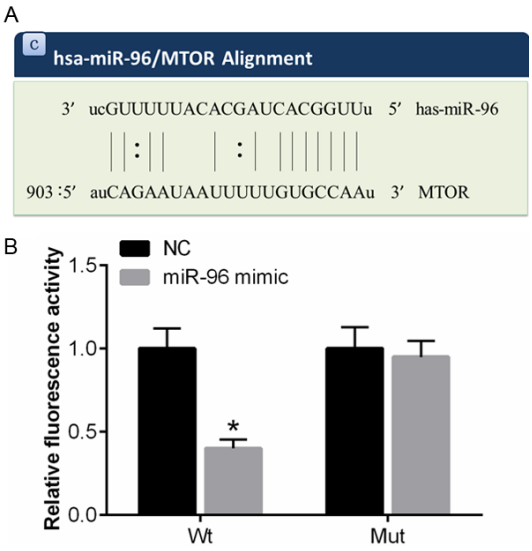

Figure 1. Verification of the target relationship between miR-96 and mTOR. A: The predicted binding site of miR-182 on mTOR 3'UTR; B: Detection result of luciferase activity. Compared with NC group, *P<0.05. miR-96, microRNA-96; NC, negative control.

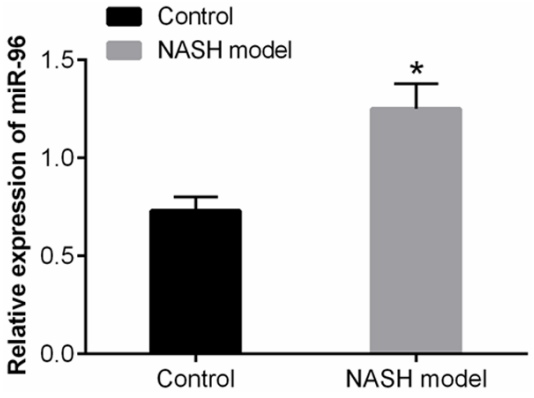

Figure 2. Expression levels of miR-96 in control group and NASH model group. Compared with the control group, *P<0.05. miR-96, microRNA-96; NASH, non-alcoholic steatohepatitis.

and mTOR 3'UTR. Thus, mTOR was the target gene of miR-96. Results of the dual fluorescent reporter gene system showed that, compared to the NC group, the luciferase signal was decreased in the Wt-miR-96/mTOR co-transfection group in the miR-96 mimic transfection group (t=7.922, P=0.001), while the mutant-type Mut-miR-96/mTOR plasmid group had no significant differences in luciferase signal (t=0.535, P=0.620). Therefore, mTOR was the target gene of miR-96 as shown in **Figure 1**.

High expression of miR-96 in a mouse model of NASH

Results of qRT-PCR detection are shown in **Figure 2**. Expression of miR-96 in the NASH model group was higher than that in the control group, with statistical differences (t=6.100, P=0.003).

qRT-PCR results and western blot results

qRT-PCR and Western blot results are shown in **Figure 3**. Compared to the blank group and NC group, expression of miR-96 mRNA was significantly increased in the miR-96 mimic group while mTOR, AKT, and S6K1 mRNA levels were significantly decreased. Expression of miR-96 mRNA was significantly decreased in the miR-96 inhibitor group while mTOR, AKT, and S6K1 mRNA levels were significantly increased (all P<0.05). Compared to the miR-96 mimic group, expression of miR-96 mRNA was significantly decreased in the miR-96 inhibitor group (t=16.430, P<0.001) while mTOR, AKT, and S6K1 mRNA levels were significantly increased (t=11.830, P<0.001; t=10.800, P<0.001; t=10.150, P<0.001). There were no statistical differences between the blank group and NC group (all P>0.05).

Compared to the blank group and NC group, mTOR, AKT, and S6K1 protein levels and their phosphoprotein levels were significantly decreased in the miR-96 mimic group. mTOR, AKT, and S6K1 protein levels and their phosphoprotein levels were significantly increased in the miR-96 inhibitor group (all P<0.05). Compared to the miR-96 mimic group, mTOR, AKT, and S6K1 protein levels and their phosphoprotein (p-mTOR, p-AKT, p70S6K1) levels were significantly increased in the miR-96 inhibitor group (t=17.730, P<0.001; t=13.020, P<0.001; t=15.370, P<0.001; t=13.370, P<0.001; t=12.080, P<0.001; t=13.140, P<0.001). There were no statistical differences between the blank group and NC group (all P>0.05).

Increased expression of mTOR in liver tissues of NASH mice

Immunohistochemistry was used to detect expression of mTOR protein in paraffin-embedded liver tissue samples of 12 mice in the NASH model group and expression of mTOR protein in

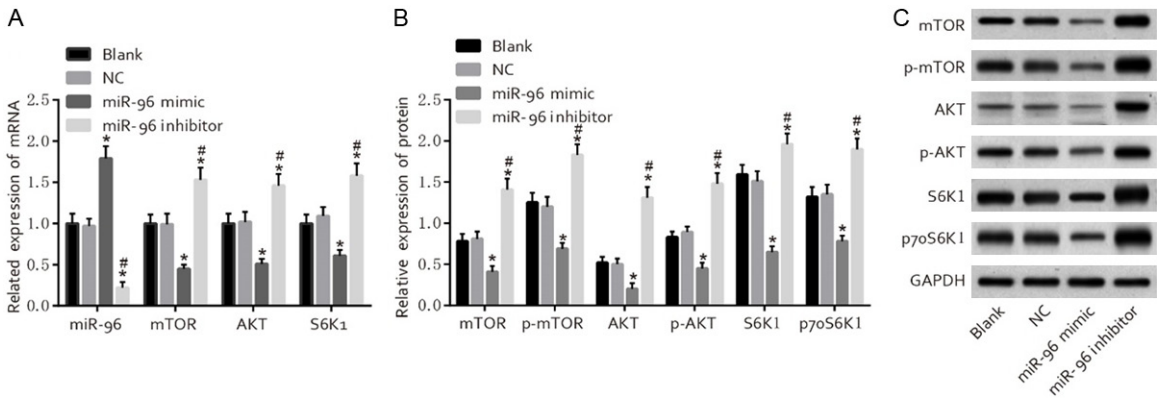

Figure 3. qRT-PCR and Western blot results of HL-7702 cells in each group. A: Relative expression of mRNA in HL-7702 cells; B: Relative expression of protein in HL-7702 cells; C: Electrophoresis band chart. Compared with the blank group and NC group, *P<0.05; compared with the miR-96 mimic group, #P<0.05. miR-96, microRNA-96; NC, negative control.

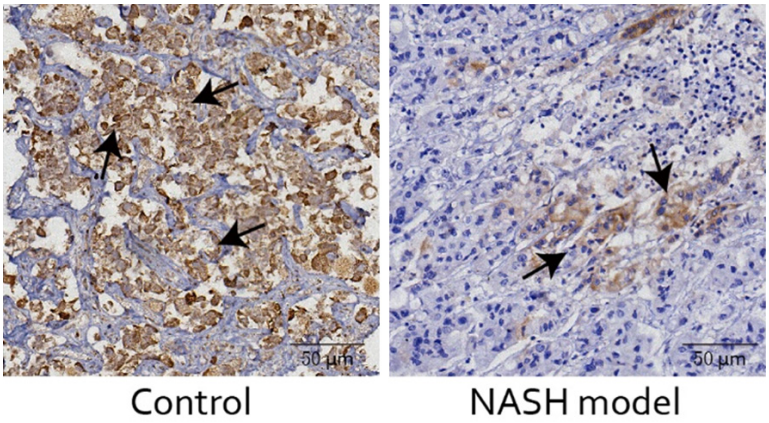

Figure 4. Immunohistochemical staining of mTOR positive cells in liver tissues of mice in each group (200×), NASH, non-alcoholic steatohepatitis.

paraffin-embedded liver tissue samples of 12 mice in the control group (**Figure 4**). mTOR expression in liver tissue of the NASH model group was significantly lower than the control group (P<0.05). Statistical results of mTOR positive cell rates are shown in **Figure 5**. mTOR positive cell rate of the NASH model group was significantly lower than the control group (P<0.05).

Cell proliferation activity in each group

MTT results are shown in **Figure 6**. There were no significant differences in the proliferation of HL-7702 cells between the blank group and NC group when cells were cultured for 24 hours, 48 hours, and 72 hours for MTT treatment (F=0.421, P=0.665). Compared to the blank group and NC group, cell proliferation rate of the miR-96 mimic group was significantly increased (F=9.159, P=0.003; F=6.614, P=0.011) and cell proliferation rate of the miR-96 inhibitor group was significantly decreased (F=4.727, P=0.030; F=6.909, P=0.010). Cell proliferation rate of the miR-96 inhibitor group was significantly lower than that of the miR-96 mimic group (F=23.660, P<0.001).

Apoptosis in each group

Hoechst staining results are shown in **Figure 7**. Nuclei were blue and evenly lightly stained, indicating that they were in normal condition. Apoptotic nuclei, exhibiting karyopyknosis and chromatin condensation, were present. Compared to the blank group and NC group, the apoptosis rate of HL-7702 cells in the miR-96 mimic group was lower (t=9.812, P<0.001; t=8.779, P<0.001) and the apoptosis rate of HL-7702 cells in the miR-96 inhibitor group was higher (t=4.850, P=0.008; t=5.543, P=0.005). There were no significant differences between the blank group and NC group (t=0.816, P=0.460). The apoptosis rate of HL-7702 cells in the miR-96 inhibitor group was higher than that of the miR-96 mimic group (t=13.380, P<0.001).

Discussion

Non-alcoholic fatty liver disease (NAFLD) is a common clinical chronic liver disease. Simple

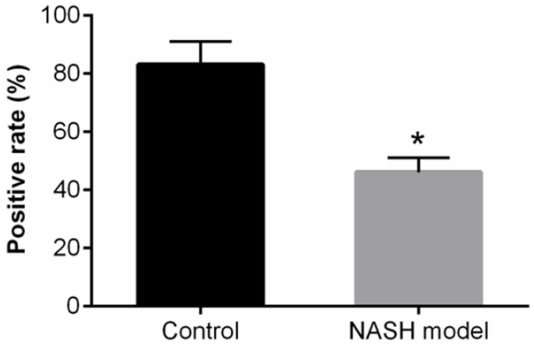

Figure 5. Comparison of the rate of mTOR positive cells in mice in each group. Compared with the control group, *t=6.793, *P=0.002. NASH, non-alcoholic steatohepatitis.

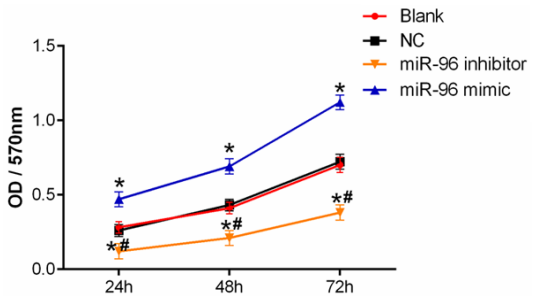

Figure 6. Comparison of cell proliferation by MTT method. Compared with the blank and NC group, *P<0.05; Compared with the miR-96 mimic group, #P<0.05. miR-96, microRNA-96; OD, optical density; NC, negative control.

fatty liver and NASH are diseases in the spectrum of NAFLD [16, 17]. One study has confirmed that NASH is a progressive state of NAFLD, likely developing into malignant diseases such as liver cirrhosis or even liver cancer [18].

MicroRNAs exist as single-stranded non-coding RNAs in humans and other eukaryotes. Studies have confirmed that they play an important role in regulation of gene expression [19]. In recent years, it has been found that miRNAs play an important role in cell differentiation, growth, proliferation, metabolism, apoptosis, tumor development, and metastasis [20]. An increasing number of studies have shown that miRNAs play an important role in the development of NAFLD. For example, miR-122 is widely present in stem cells. It accounts for approximately 50% of the total miRNA in the liver [21]. MicroRNA can regulate the growth and differentiation of human cells as well as regulate the metabolism of liver and energy. Some studies have found that miRNAs are also involved in oxidative stress, inflammation, and apoptosis in the liver, along with endoplasmic reticulum stress [22]. The use of miRNAs as targets for treatment of liver diseases has also gradually attracted the attention of the medical community.

This present study established a NASH mouse model. It was found that miR-96 expression in liver tissue of NASH mice was significantly higher than that of normal mice (all P<0.05), suggesting an association between miR-96 and NASH. Some studies have investigated the effects of miRNA therapy on obesity, fatty liver, and other diseases, finding that the effects of inhibiting the miR-96 expression are more pronounced than traditional hypoglycemic, lipid-lowering, and weight-reducing drugs [23, 24]. This further confirms that miR-96 plays a role in occurrence and development of NASH. This study proves that AKT/mTOR signaling pathways are an important controller for the human body. They regulate cell growth, differentiation, proliferation, and apoptosis. They also play an important role in human biological functions [25]. To further investigate specific mechanisms of miR-96 in the pathogenesis of NASH, this study used qRT-PCR and Western blot to detect mRNA and protein expression in the cells of each group. Results showed that miR-96 protein and mRNA levels of the miR-96 mimic group were significantly higher than those of the miR-96 inhibitor group. mTOR, AKT, and S6K1 protein and mRNA levels of the miR-96 mimic group were significantly lower than those of the miR-96 inhibitor group (all P<0.05). Analysis by on-line analysis software and dual-luciferase reporter assays showed that binding sites existed between miR-96 and mTOR 3'UTR and that mTOR was a target gene of miR-96. Proliferation and apoptosis of HL-7702 cells in each group were observed by MTT and Hoechst staining. It was found that, compared with the blank group and NC group, the proliferation rate of the miR-96 mimic group was significantly higher and the apoptosis rate of HL-7702 cells in the miR-96 mimic group was lower while the apoptosis rate of HL-7702 cells in the miR-96 inhibitor group was higher (all P<0.05). These results suggest that miR-96 regulates proliferation and apo-

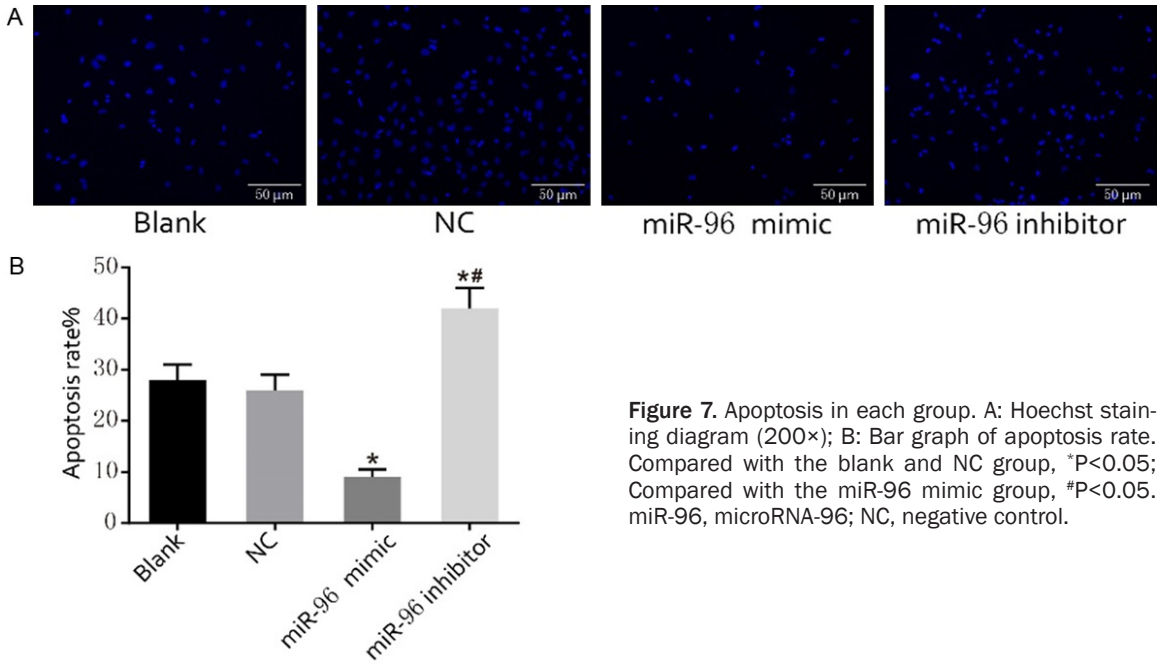

Figure 7. Apoptosis in each group. A: Hoechst staining diagram (200×); B: Bar graph of apoptosis rate. Compared with the blank and NC group, *P<0.05; Compared with the miR-96 mimic group, #P<0.05. miR-96, microRNA-96; NC, negative control.

ptosis of hepatocytes. Results of immunohistochemistry showed that expression of mTOR protein in the liver tissues of the NASH model group was significantly lower than that of the control Group. mTOR-positive cell rate was also significantly decreased (all P<0.05), suggesting that miR-96 regulates NASH mainly through affecting AKT/mTOR signaling pathways. Some studies have investigated the roles of AKT/mTOR signaling pathways in the progression of liver cancer. They have found that mTOR is an important factor in the regulation of energy and substance metabolism in the human body, playing an important role in the life activities of cells [26]. Therefore, it was speculated that impact on the pathogenesis of NASH may also be exerted in the growth and metabolism of cells and activation of human protein kinases, along with other factors. In this study, mechanisms of miR-96 affecting non-alcoholic fatty liver were explored from the perspective of genes and signaling pathways. However, further relevant *in vivo* experiments and toxicity tests are necessary.

In summary, miR-96 plays an important role in the pathogenesis of NASH. High expression of miR-96 can inhibit AKT/mTOR signaling pathways, promote proliferation of NASH cells, and reduce apoptosis. miR-96 can be used as an important future target for treatment of NASH.

Acknowledgements

This work was supported by Shandong Provincial Natural Science Foundation (ZR2014HM-081) and Shandong Provincial Medical and Health Science and Technology Development Plan Project (2015WS0378).

Disclosure of conflict of interest

None.

Address correspondence to: Likun Wang, Department of Infectious Diseases, Linyi People's Hospital, No. 27 Jiefang Road, Lanshan District, Linyi 276000, Shandong Province, China. Tel: +86-0539-8097172; E-mail: wanglikun58hr@163.com

References

[1] Hachemi M, Benmakhlouf S, Prost P, Santolaria N, Tchenio X, Sedillot N and Zoulim F. Non alcoholic fatty liver disease and Non alcoholic steato-hepatitis are multisystemic diseases: review for intensivists. Médecine Intensive Réanimation 2017; 26: 63-74.

[2] Safaei A, Oskouie AA, Mohebbi SR, Rezaeitavirani M, Mahboubi M, Peyvandi M, Okhovatian F and Zamanianazodi M. Metabolomic analysis of human cirrhosis, hepatocellular

carcinoma, non-alcoholic fatty liver disease and non-alcoholic steatohepatitis diseases. Gastroenterol Hepatol Bed Bench 2016; 9: 158-173.

[3] Mauro SD, Ragusa M, Urbano F, Filippello A, Pino AD, Scamporrino A, Pulvirenti A, Ferro A, Rabuazzo AM and Purrello M. Intracellular and extracellular miRNome deregulation in cellular models of NAFLD or NASH: clinical implications. Nutr Metab Cardiovasc Dis 2016; 26: 1129.

[4] Szabo G and Csak T. Role of MicroRNAs in NAFLD/NASH. Dig Dis Sci 2016; 61: 1314-1324.

[5] Hartig SM, Hamilton MP, Bader DA and Mcguire SE. The miRNA interactome in metabolic homeostasis. Trends Endocrinol Metab 2015; 26: 733-745.

[6] Tilg H, Moschen AR and Szabo G. Interleukin-1 and inflammasomes in alcoholic liver disease/acute alcoholic hepatitis and nonalcoholic fatty liver disease/nonalcoholic steatohepatitis. Hepatology 2016; 64: 955-965.

[7] Liu XL, Pan Q, Zhang RN, Shen F, Yan SY, Sun C, Xu ZJ, Chen YW and Fan JG. Disease-specific miR-34a as diagnostic marker of non-alcoholic steatohepatitis in a Chinese population. World J Gastroenterol 2016; 22: 9844-9852.

[8] Yu K, Li N, Cheng Q, Zheng J, Zhu M, Bao S, Chen M and Shi G. miR-96-5p prevents hepatic stellate cell activation by inhibiting autophagy via ATG7. J Mol Med (Berl) 2017; 96: 65-74.

[9] Chandel R, Das A, Chawla YK and Kaur J. Mo1477 progression of hepatocellular carcinoma is associated with the up regulation of rno-miR-96/182/183 cluster in liver of wistar rats. Gastroenterology 2016; 150: S1125-S1125.

[10] Goldberg D, Ditah IC, Saeian K, Lalehzari M, Aronsohn A, Gorospe EC and Charlton M. Changes in the prevalence of hepatitis C virus infection, nonalcoholic steatohepatitis, and alcoholic liver disease among patients with cirrhosis or liver failure on the waitlist for liver transplantation. Gastroenterology 2017; 152: 1090-1099.

[11] Afonso MB, Rodrigues PM, Simão AL and Rui EC. Circulating microRNAs as potential biomarkers in non-alcoholic fatty liver disease and hepatocellular carcinoma. J Clin Med 2016; 5: 30.

[12] Wang TH, Yeh CT, Ho JY, Ng KF and Chen TC. OncomiR miR-96 and miR-182 promote cell proliferation and invasion through targeting ephrinA5 in hepatocellular carcinoma. Mol Carcinog 2016; 55: 366-375.

[13] Iyer S, Upadhyay PK, Majumdar SS and Nagarajan P. Animal models correlating immune cells for the development of NAFLD/NASH. J Clin Exp Hepatol 2015; 5: 239.

[14] Han C, Wei S, He F, Liu D, Wan H, Liu H, Li L, Xu H, Du X and Xu F. The regulation of lipid deposition by insulin in goose liver cells is mediated by the PI3K-AKT-mTOR signaling pathway. PLoS One 2015; 10: e0098759.

[15] Liu BF, Zhou DS, Liang ZQ and Bai JH. Effects of artesunate on hepatic NF-κB and TNF-α in mice with non-alcoholic fatty liver. Pharmacology and Clinics of Chinese Materia Medica 2014; 23-26.

[16] Zhao JX, Yuan YW, Cai CF, Shen DY, Chen ML, Ye F, Mi YJ, Luo QC, Cai WY and Zhang W. Aldose reductase interacts with AKT1 to augment hepatic AKT/mTOR signaling and promote hepatocarcinogenesis. Oncotarget 2017; 8: 66987-67000.

[17] Smith BW and Adams LA. Non-alcoholic fatty liver disease. Crit Rev Clin Lab Sci 2011; 48: 97-113.

[18] Mikako O and Hirofumi N. Diagnosis and evaluation of nonalcoholic fatty liver disease. Exp Diabetes Res 2012; 2012: 145754.

[19] Li J, Li X, Xu W, Wang S, Hu Z, Zhang Q, Deng X, Wang J, Zhang J and Guo C. Antifibrotic effects of luteolin on hepatic stellate cells and liver fibrosis by targeting AKT/mTOR/p70S6K and TGFβ/Smad signalling pathways. Liver Int 2015; 35: 1222-1233.

[20] Tang H, Li RP, Liang P, Zhou YL and Wang GW. miR-125a inhibits the migration and invasion of liver cancer cells via suppression of the PI3K/AKT/mTOR signaling pathway. Oncol Lett 2015; 10: 681.

[21] Pierobon M, Ramos C, Wong S, Hodge KA, Aldrich J, Byron S, Anthony SP, Robert NJ, Northfelt DW and Jahanzeb M. Enrichment of PI3K-AKT-mTOR pathway activation in hepatic metastases from breast cancer. Clin Cancer Res 2017; 23: 4919-4928.

[22] Li C, Yang W, Zhang J, Zheng X, Yao Y, Tu K and Liu Q. SREBP-1 has a prognostic role and contributes to invasion and metastasis in human hepatocellular carcinoma. Int J Mol Sci 2014; 15: 7124-7138.

[23] Yang WM, Min KH and Lee W. Induction of miR-96 by dietary saturated fatty acids exacerbates hepatic insulin resistance through the suppression of INSR and IRS-1. PLoS One 2016; 11: e0169039.

[24] Assal RA, El Tayebi HM, Hosny KA, Esmat G and Abdelaziz AI. A pleiotropic effect of the single clustered hepatic metastamiRs miR-96-5p and miR-182-5p on insulin-like growth factor II, insulin-like growth factor-1 receptor and insulin-like growth factor-binding protein-3 in hepa-

tocellular carcinoma. Mol Med Rep 2015; 12: 645.

[25] Koufaris C, Wright J, Currie RA and Gooderham NJ. Hepatic microRNA profiles offer predictive and mechanistic insights after exposure to genotoxic and epigenetic hepatocarcinogens. Toxicol Sci 2012; 128: 532-543.

[26] Takaki Y, Saito Y, Takasugi A, Toshimitsu K, Yamada S, Muramatsu T, Kimura M, Sugiyama K, Suzuki H and Arai E. Silencing of microRNA-122 is an early event during hepatocarcinogenesis from non-alcoholic steatohepatitis. Cancer Sci 2014; 105: 1254-1260.